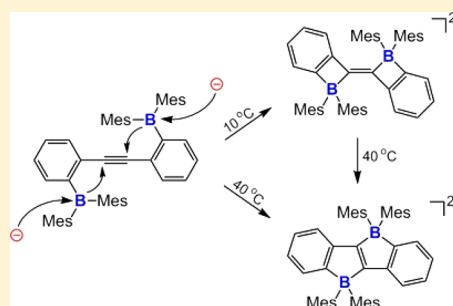


Synthesis of Bis-Cycloborate Olefin and Butatriene Derivatives through the Reduction of Alkynyl-Bridged Diboryl Compounds

Jinyu Zhao,^{†,§} Chenglong Ru,^{†,§} Yunfei Bai,[†] Xingyong Wang,^{*,‡,§} Wenhao Chen,[†] Xi Wang,[†] Xiaobo Pan,^{*,†,§} and Jincai Wu^{†,§}[†]State Key Laboratory of Applied Organic Chemistry, Key Laboratory of Nonferrous Metal Chemistry and Resources Utilization of Gansu Province, College of Chemistry and Chemical Engineering, Lanzhou University, Lanzhou 730000, P. R. China[‡]School of Chemistry, University of Wollongong, Wollongong, NSW 2522, Australia

Supporting Information

ABSTRACT: A series of bis-cycloborate olefin and butatriene derivatives were synthesized from alkynyl-bridged diboryl compounds using a simple reduction strategy. In the reduction route of 1,2-bis[2-(dimesitylboryl)phenyl]ethyne (1), bis-cycloborate olefin (4) to diborate-bridged stilbene (5) can be obtained selectively by varying the reaction temperature. In addition, a thermal isomerization from 4 to 5 was found as a result of the rearrangement of double bonds. The generality of this reaction was further verified in similar reduction reactions. In the direduction of 1,2-bis[8-(dimesitylboryl)naphthalen-1-yl]ethyne (2), the bis-cycloborate olefin (6) was isolated in high yield and demonstrated no thermal isomerization. In the two-electron reduction of 1,8-bis[2-(dimesitylboryl)phenyl]ethynyl naphthalene (3), the bis-cycloborate butatriene (7) was obtained unexpectedly because of the departure of the naphthyl group. When using Na as the reductant and diethyl ether as the solvent, 1,2-bis[(Z)-2-(dimesitylboryl)benzylidene]-1,2-dihydroacenaphthylene (8) was isolated after adding 1 or 2 drops of H₂O to the reduction reaction filtrates. Meanwhile, the related mechanisms for radical cyclization, thermal isomerization, and formation of bis-cycloborate butatriene were also discussed.



INTRODUCTION

Boron-containing compounds have attracted a great deal of attention because of their potential applications in luminescent organic materials,^{1–11} anion sensors,^{12–15} photochemistry,^{16–18} and polyaromatic hydrocarbon chemistry.^{19–23} Triarylboron compounds have excellent electron accepting properties because of the low-lying empty p orbital of the boron atom. Recently, numerous single-electron-reduced species, including boron-stabilized anions^{24,25} and radical anions,^{26–32} were synthesized by the reduction method under different conditions, and this strategy has already become a hot research topic. However, as an important part of boron reduction chemistry, the direduction behaviors of diboryl-substituted compounds have been studied less.

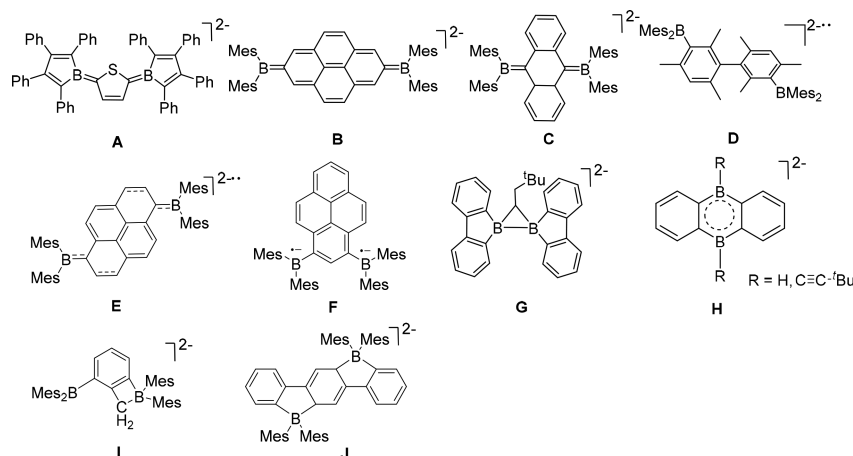
Continuous efforts have led to the emergence of different direduction results. Braunschweig, Marder, and our group displayed the synthesis of three quinoidal dianions, A,³³ B,³⁴ and C³⁵ (Scheme 1), upon two-electron reduction of 2,5-bis(borolyl)thiophene, 2,7-bis(BMes₂)pyrene, and 9,10-bis(dimesitylboryl)anthracene, respectively. Wang and co-workers showed the formation of three diradical dianions D–F^{36,37} (Scheme 1) through direduction and discussed their structures and spectroscopic properties. Wagner and co-workers reported the two-electron trap process of bis(9-borafluorenyl)methane and 9,10-diboraanthracene derivatives, which led to the formation of a B–B σ bond (G³⁸) and the dianionic H³⁹ (Scheme 1). Recently, Wang et al.³⁶ and our group⁴⁰

demonstrated the preparation of cyclic borate structures via an elegant two-electron reduction path. In addition to the structural exploration of these compounds, utilizing such a synthetic method to build new functional boron-containing skeletons is also very important, which has been, however, explored less.

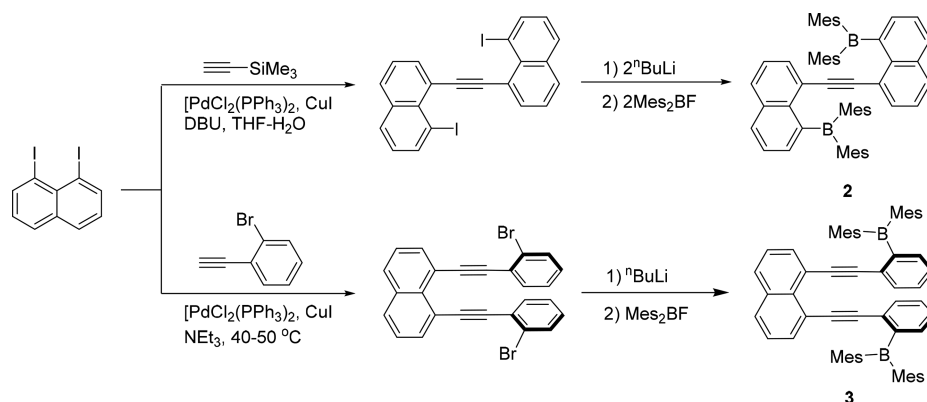
By using this reduction strategy, we recently succeeded in reducing 9,10-bis(dimesitylboryl)anthracene and *o*-dimesitylboryl-substituted compounds. These results,^{35,40} especially the reduction of *o*-dimesitylboryl-substituted compounds, encouraged us to investigate the reduction behaviors of other similar boron-containing systems. In this paper, we demonstrate the reduction of alkynyl-bridged diboryl compounds and discuss the spectroscopic character and crystal structures of their reduced products. Meanwhile, a thermal isomerization process from bis-cycloborate olefin 4 to diborate-bridged stilbene 5 due to the rearrangement of double bonds was observed. In addition, the bis-cycloborate butatriene {K⁺[2.2.2]-cryptand}₂·7a^{2–} (7) was obtained unexpectedly because of the departure of the naphthyl group, which was attributed to the effect of “extrusion reaction”, while compound 8 was isolated after adding 1 or 2 drops of H₂O to the filtrates when using Na as the reductant and diethyl ether as the solvent in the two-electron reduction of 3.

Received: June 5, 2018

Scheme 1. Structurally Characterized Diboryl Dianions A–J



Scheme 2. Synthesis of Compounds 2 and 3



RESULTS AND DISCUSSION

Synthesis, Structure, and Characterization of Compounds 1–3. The known 1,2-bis[2-(dimesitylboryl)phenyl]ethyne (**1**) was synthesized according to Aldridge's work.⁴¹ Compounds 1,2-bis[8-(dimesitylboryl)naphthalen-1-yl]ethyne (**2**) and 1,8-bis[[2-(dimesitylboryl)phenyl]ethynyl]naphthalene (**3**) (Scheme 2) were prepared from the reaction between the ⁿBuLi-lithiated corresponding halogenated aromatic compounds in tetrahydrofuran (THF) and 2 equiv of Mes₂BF at −78 °C. They were isolated as colorless solids by column chromatography with a 10:1 mixture of CH₂Cl₂ and hexanes as the eluent in 69 and 64% yields, respectively. They are stable toward moisture and air and display blue fluorescence when irradiated under 365 nm ultraviolet (UV) light both in solution and in the solid state. All compounds were further analyzed by multinuclear nuclear magnetic resonance (NMR) spectroscopy. The ¹¹B NMR resonances of compounds **1–3** appear at 75 (73⁴¹), 65.7, and 74.1 ppm, respectively, which are comparable to those reported for two coordinated boron compounds [2,7-bis-(BMes₂)pyrene, 75.3 ppm,³⁴ and 2,6-bis(BMes₂)mesitylene, 74.8 ppm³⁶], as well as our reported *o*-dimesitylboryl-substituted compound (75 ppm).⁴⁰ In the ¹³C NMR spectra of compounds **1–3**, the peaks at 93.5 ppm (in **1**), 100.5 ppm (in **2**), and 97.6 and 93.2 ppm (in **3**) confirm the existence of alkyne carbons. It is worth noting that a broad peak appears at 1.53 ppm in the ¹H NMR spectrum of **2**, which is likely due to hindered rotation of the Mes groups in very constricted

environments. In addition, the structures of compounds **1–3** were further verified by X-ray diffraction (Figure 1a–c). Interestingly, the alkyne bonds are considerably bent, with bending angles of up to 169.9(5)° (C2–C1–C1') in **1**, 160.9(4)° (C2–C1–C1') in **2**, and 170.6(3)° (C27–C26–C1) and 164.8(2)° (C35–C37–C38) in **3**, which may be caused by the crowded Mes groups.

To study the redox properties of compounds **1–3**, cyclic voltammetry was performed in THF with ⁿBu₄NPF₆ as the supporting electrolyte, and they exhibited quite different features (Figure 1d). Two distinct sets of quasi-reversible reduction waves were observed in compounds **1** (*E*_{1/2} = −2.07 V and *E*_{1/2} = −1.80 V vs Fc/Fc⁺) and **3** (*E*_{1/2} = −2.42 V and *E*_{1/2} = −2.13 V vs Fc/Fc⁺), while two irreversible reduction waves were found at *E*_{pc} = −2.24 V and *E*_{pc} = −1.78 V versus Fc/Fc⁺ in compound **2**. Generally, two reversible reduction waves could appear in the reduction system of diboryl compounds. The first reduction wave corresponds to the formation of a monoradical anion in which the unpaired electron occupies a molecular orbital bearing large contributions from that of the boron p orbitals,⁴² while the second reduction wave corresponds to the formation of a dianion, which exists either as a biradical or as a σ-bonded derivative. According to our previous studies,⁴⁰ the redox behaviors compounds **1–3** most likely indicate a significant structural change associated with the electron-transfer process.⁴³

Synthesis, Structure, and Characterization of Complexes 4 and 5. Inspired by the electrochemical results presented above, we investigated the chemical reduction of **1**

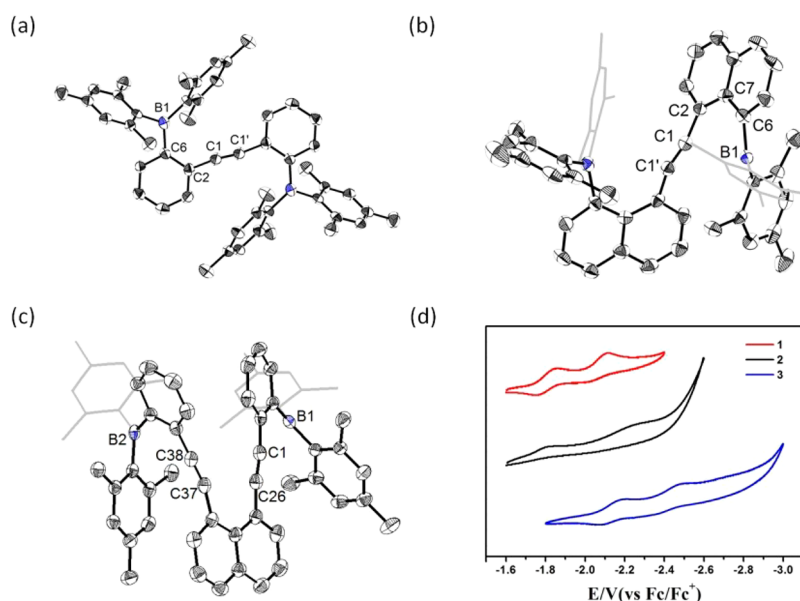
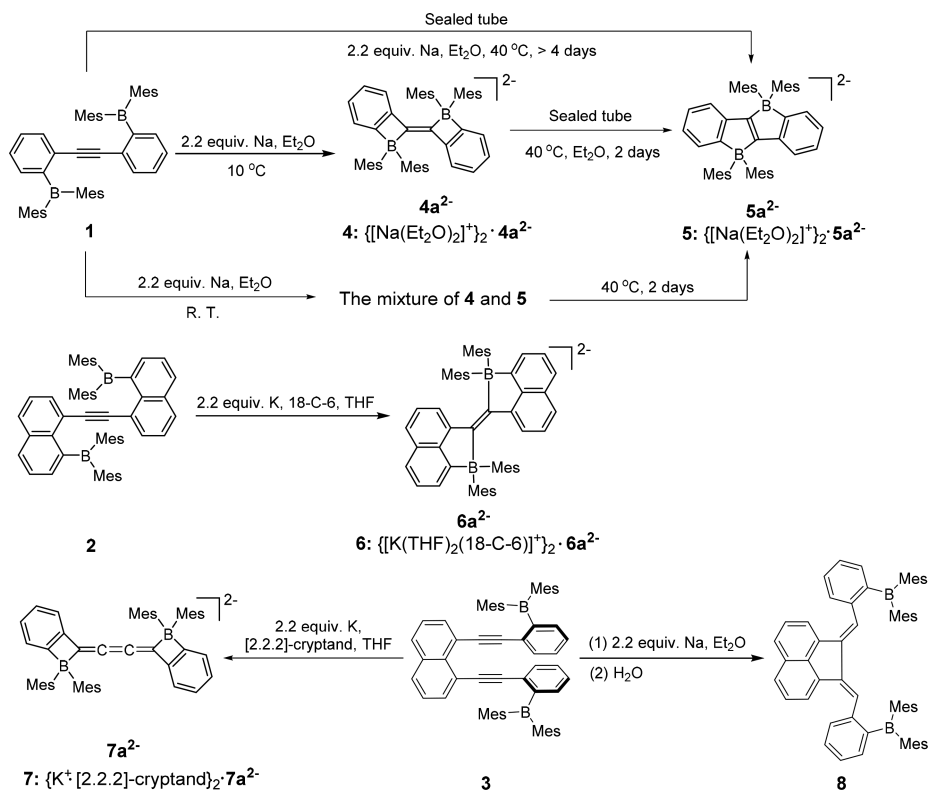


Figure 1. Thermal ellipsoid (50%) drawings of compounds 1–3. All H atoms have been omitted for the sake of clarity. Selected bond lengths (angstroms) and bond angles (degrees): (a) in 1, C1–C1' 1.186(6), C1–C2 1.432(4), C6–B1 1.572(5), C8–B1 1.589(5), C17–B1 1.572(5), C1'–C1–C2 169.9(5), C6–B1–C8 114.5(3), C6–B1–C17 124.0(3), C17–B1–C8 121.4(3); (b) in 2, C1–C1' 1.197(7), C1–C2 1.435(4), C6–B1 1.575(5), C12–B1 1.555(6), C21–B1 1.572(6), C1'–C1–C2 160.9(4), C12–B1–C6 124.0(4), C12–B1–C21 120.2(3), C21–B1–C6 114.7(3); and (c) in 3, C1–C26 1.207(4), C37–C38 1.205(3), C6–B1 1.573(4), C8–B1 1.580(4), C17–B1 1.574(4), C44–B2 1.570(4), C45–B2 1.581(4), C54–B2 1.579(4), C1–C2 1.430(4), C35–C37 1.441(4), C38–C39 1.443(4), C26–C1–C2 173.1(3), C27–C26–C1 170.6(3), C39–C38–C37 176.8(2), C38–C37–C35 164.8(2), C17–B1–C6 123.3(2), C17–B1–C8 123.7(2), C45–B2–C44 117.6(2), C54–B2–C45 118.6(2), C54–B2–C45 123.7(2). (d) Cyclic voltammograms of compounds 1–3 (5×10^{-4} M) in THF, containing 0.1 M Bu_4NPF_6 , measured at 100 mV s^{-1} and room temperature.

Scheme 3. Synthesis of Compounds 4–8



in fresh distilled Et_2O (Scheme 3). First, the reaction was performed at room temperature, which leads to the formation of a yellow solid in 73% yield. The ^1H NMR spectrum shows a

complex (Figure S14) but nicely resolved signal. The enlarged signals of aromatic hydrogens (Figure 2b) in the ^1H NMR spectrum can be identified as the resonances of complexes 4

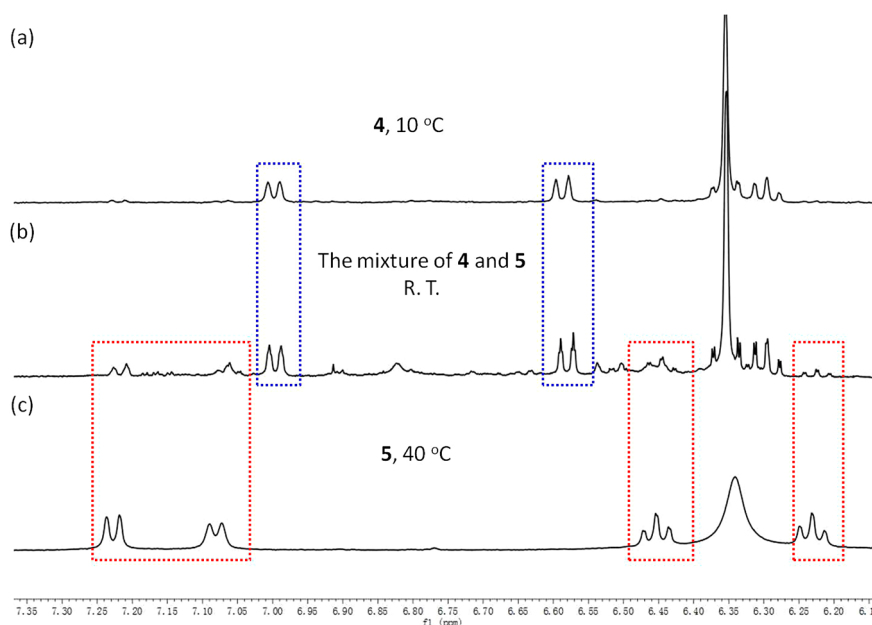


Figure 2. Enlarged signals of aromatic hydrogens of complexes **4** and **5**. They were obtained from reduction of **1** at different reaction temperatures: (a) 10 °C, (b) room temperature, and (c) 40 °C.

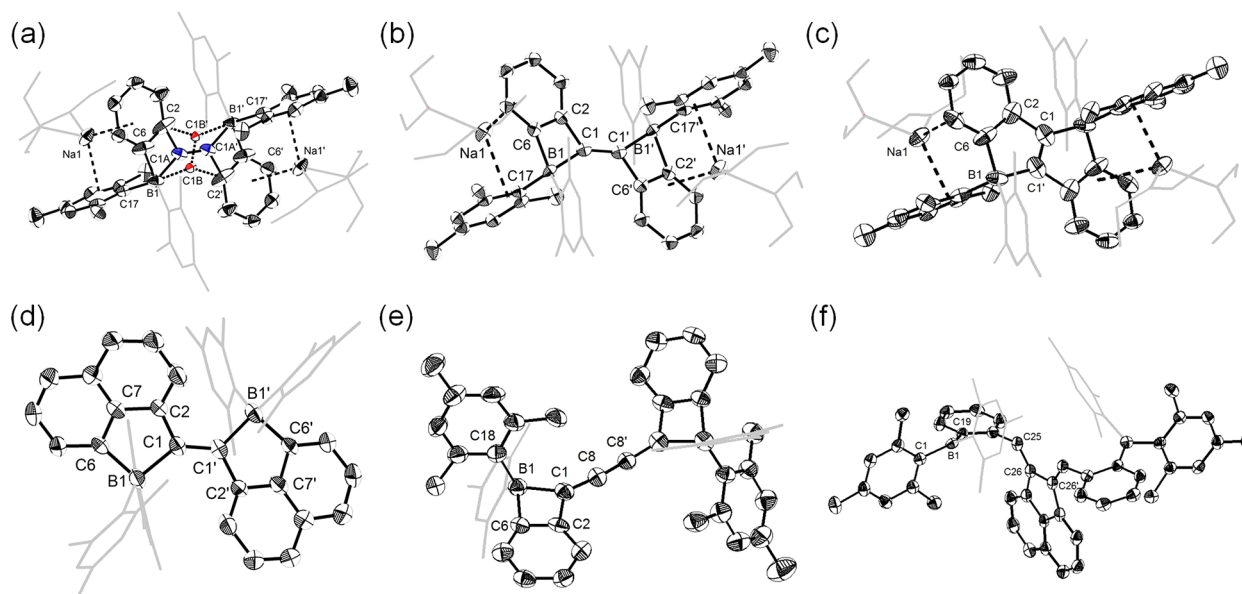
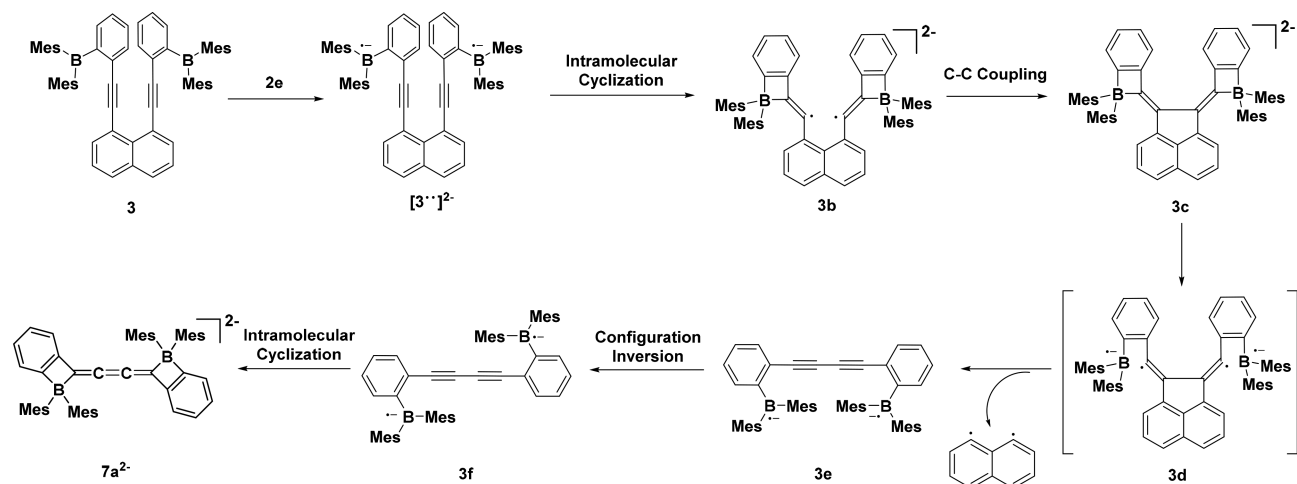


Figure 3. Thermal ellipsoid (50%) drawings of products **4**–**8**: (a) mixture of **4** and **5**, (b) **4**, (c) **5**, (d) **6**, (e) **7**, and (f) **8**. Free molecules and all H atoms have been omitted for the sake of clarity. Selected bond lengths (angstroms): in **4**, B1–C1 1.704(4), C1–C2 1.477(4), C1–C1' 1.347(5); in **5**, B1–C1' 1.669(2), C1–C2 1.488(2), C1–C1' 1.353(3); in **6**, C1–C1' 1.362(10), C1–B1 1.764(7), C2–C1 1.472(7); in **7**, B1–C1 1.696(14), B1–C6 1.665(16), C1–C2 1.476(14), C1–C8 1.328(12), C8–C8' 1.24(2); in **8**, C1–B1 1.585(3), C24–C25 1.486(3), C25–C26 1.340(3), C26–C26' 1.510(3).

and **5**, indicating the yellow solid is a mixture of complexes **4** and **5**. In addition, single-crystal X-ray diffraction (Figure 3a) studies at -5°C further showed it consists of two configurations: bis-cycloborate olefin **4** and diborate-bridged stilbene **5**. Subsequently, to avoid the formation of the mixture product, the reaction was again performed at two different temperatures, 10 and 40 °C (Scheme 3). Then the two reaction solutions were filtered and concentrated in vacuum. Finally a light yellow solid **4** and a golden yellow solid **5** were isolated in 58 and 87% yields, respectively. Their ^{11}B NMR resonances appear at -3.81 and -7.98 ppm, respectively, which are significantly shifted downfield compared to that of

compound **1** and close to those reported for coordinated boron compounds.^{40,44,45} In addition, in the ^{13}C NMR spectra, the disappearance of alkyne carbons' signals further indicates the formation of complexes **4** and **5**. The chemical shifts in the ^1H NMR spectra for complexes **4** and **5** are distinctly different (Figure 2a,c). For example, the aromatic peak (7.00 ppm) in the lowest field of complex **4** is obviously lower than that of complex **5** (7.23 ppm). These results demonstrate that complexes **4** and **5** are clearly different and can be obtained selectively by varying the reaction temperature. Moreover, we also found complex **4** can convert to complex **5** completely when the solution of complex **4** is heated at 40 °C for 2 days in

Scheme 4. Proposed Mechanism for the Formation of 7



a sealed tube. This isomerization is a thermally driven process, which is different from the light-driven and acid-induced isomerization of Pier^{46,47} and Barton.⁴⁸ Meanwhile, density functional theory (DFT) calculations (see below) further show that stilbene **5** is 32.1 kcal mol^{−1} more stable than isomer **4**. In addition, the isolated mixture described above that was obtained at room temperature also completely converted to complex **5** when its Et₂O solution was heated at 40 °C. All these experiments clearly show that complex **5** is a thermodynamic product.

Crystals of complexes **4** and **5** suitable for single-crystal X-ray diffraction were obtained in an Et₂O solution at −25 °C. Panels b and c of Figure 3 display their solid structures. Their important structural parameters are listed in Table S2. According to X-ray diffraction, they display bis-cycloborate olefin (**4**) and diborate-bridged stilbene (**5**) structures, respectively. Complex **4** features a structure with two four-membered boracycles linked by a C=C bond [1.347(5) Å], and the boron atoms are in a trans arrangement about the double bond. The B1–C1 (or B1'–C1') bond length [1.704(4) Å] is close to that of the previous counterpart **J** [1.710(5) Å].⁴⁰ In complex **5**, the newly formed B1–C1' (or B1'–C1) bond leads to the formation of a five-membered ring-fused borate geometry. The B1(B1')–C1'(C1) bond length [1.669(2) Å] is close to those of previously reported compounds **SA–SC** [1.665(3) Å,⁴⁴ 1.645(3) Å,⁴⁵ and 1.670(7) Å,⁴⁹ respectively (Scheme S1)] but shorter than that of **SD** [1.842(3) Å (Scheme S1)].⁵⁰ The skeleton is nearly planar, which is reflected in torsion angles C6–C2–C1–C1' (7.84°), C2–C1–C1'–C2' (0°), and C1–C1'–C2–C6 (7.84°). Besides being coordinated to two Et₂O molecules, each Na⁺ ion in complexes **4** and **5** is involved in cation– π bonding to phenyl moieties and Mes units. In addition, the structure of **5** is similar to those of phosphonium- and borate-bridged zwitterionic stilbenes that were synthesized by intramolecular cascade cyclization.^{51,52}

Synthesis, Structure, and Characterization of Compounds 6–8. To further explore the generality of this synthetic methodology, more extended homologues derivatives were prepared. Treatment of **2** with K chips in the presence of 18-crown-6 at room temperature afforded the complex {[K(THF)₂(18-C-6)]⁺}₂·**6a**^{2−} (**6**) in 73% yield (Scheme 3). The structure of the product was ascertained by multinuclear NMR spectroscopy, X-ray diffraction, and elemental analysis.

The ¹¹B NMR resonance of complex **6** appears at −4.16 ppm, which is significantly shifted downfield compared to that of **2** (65.7 ppm) but close to those of complexes **4** and **5**, indicating the formation of a tetracoordinate borate salt. Meanwhile, compared to precursor **2**, more broad peaks appear in the range of 6.01–6.49 ppm (Mes-*H*) and 2.03–2.35 ppm (Mes-CH₃) in the ¹H NMR spectrum of **6**, which may be caused by the hindered rotation of the Mes groups in more constricted environments. In addition, although the synthesis of complex **6** uses the same path as complex **4**, it demonstrates no thermal isomerization. The butatriene dianion {K⁺·[2.2.2]-cryptand}₂·**7a**^{2−} (**7**) was obtained (Scheme 3) unexpectedly in 43% yield upon treatment of **3** with K chips in the presence of [2,2,2]-cryptand at room temperature. The ¹¹B NMR resonance at −2.50 ppm is close to those of complexes **4**–**6**, implying the formation of a similar tetracoordinate borate structure. The ¹³C NMR spectrum was not obtained because of the poor solubility of complex **7**. The byproducts are complex, but we succeeded in identifying the structure of one main byproduct as 1,1'-dinaphthyl (Figure S21). The naphthyl signals disappear in the ¹H NMR spectrum of **7**, supporting the departure of naphthalene derivatives after the reduction of **3**.

Crystals suitable for X-ray studies were obtained from a THF solution. Despite repeated attempts, the quality of the crystals of **6** and **7** was still not good enough. The uncertainties are relatively large and allow for only a qualitative discussion. The structures of complexes **6** and **7** revealed some interesting features (Figure 3d,e). Similar to complex **4**, complex **6** shows a bis-naphthocycloborapentylidene structure linked by a C=C bond. The B1–C1 bond [1.764(7) Å] is longer than those in complexes **4** [1.704(4) Å] and **5** [1.669(2) Å]. Although all carbons are sp²-hybridized, the B₂C₈ core is not planar because of the severe angulation of the C=C bond caused by the space extrusion of crowded Mes groups. This also causes the inclination of the two naphthocycloborate fragments with a dihedral angle of ≤30.4°. Meanwhile, this crowded environment further illustrates the broadening of Mes NMR signals. Complex **7** displays a bis-cycloborate structure with two discrete borate four-membered rings linked by a butatriene fragment. The two boron centers adopt trans dispositions. The cumulene linkage is essentially linear with a C–C–C angle of 171.3(5)°, which is similar to those of the dizwitterion phosphonium borate molecules.⁵³

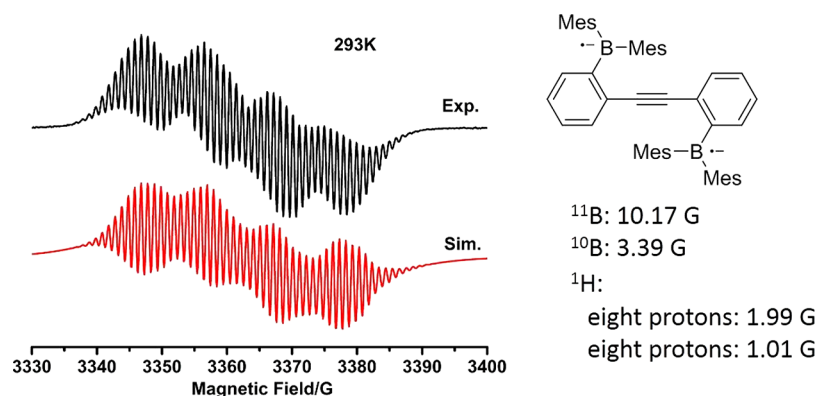


Figure 4. Experimental and simulated EPR spectra of $[1^{\bullet\bullet}]^{2-}$ and hyperfine coupling.

The previous works⁵⁴ by Power show that a different combination of reduced metals and solvents would lead to different reduction species. On the basis of this work, we tried to use Na as the reductant and diethyl ether as the solvent but failed to isolate the product. However, a large amount of solid **8** was obtained immediately in 21% yield upon adding **1** or **2** drops of H_2O to the reduction reaction filtrates. The ^{11}B NMR resonance at 70.0 ppm implies the formation of a typical three-coordinated organoboron compound, which is close to those of compounds **1**–**3**. The chemical shift of the 1H NMR spectrum at 6.12 ppm shows the formation of alkene hydrogens. Although it is difficult to unambiguously determine the backbone structure of **8** from the spectroscopic data, X-ray measurements confirmed its structure (Figure 3f), which is a typical bis-dimesitylboryl-substituted naphthalene. Two symmetrical double bonds [1.340(3) Å] replaced the previous two triple bonds [1.207(4) and 1.205(3) Å] in **3** due to the formation of the C26–C26' bond [1.510(3) Å]. The two extra hydrogen atoms in **8** were probably derived from H_2O as its addition led to the immediate appearance of **8**.

Proposed Mechanism of Formation for Complexes 4–7. To better understand these reduction reactions, electron paramagnetic resonance (EPR) measurements and DFT calculations were performed. Possible mechanisms for the formation of complexes **4**, **5**, and **7** (Scheme 4 and Scheme S2) were proposed. Although we tried to capture the EPR spectra of all proposed intermediate radicals at room temperature, only the spectrum of $[1^{\bullet\bullet}]^{2-}$ was obtained. Even if we changed the collection conditions, the EPR signals of $[2^{\bullet\bullet}]^{2-}$ and $[3^{\bullet\bullet}]^{2-}$ were still not observed. The X-band EPR spectra of $[1^{\bullet\bullet}]^{2-}$ in a THF solution show a complex but resolved signal [Figure 4; $g = 2.004$, $a(^{11}B) = 10.17$ G, $a(^{10}B) = 3.39$ G, $a(H_1) = 1.99$ G, $a(H_2) = 1.01$ G], and no half-field signal or zero-field splitting was observed (Figure S1), indicating the formation of a biradical dianion with rather weak spin–spin couplings between the two boron radical centers.⁴⁰ To further understand the electronic structures of $[1^{\bullet\bullet}]^{2-}$ – $[3^{\bullet\bullet}]^{2-}$, DFT calculations were carried out at the UCAM-B3LYP/6-31G(d) level of theory. Both the open-shell singlet (OS) and triplet (T) states were considered. $[1^{\bullet\bullet}]^{2-}$ features a singlet ground state with a singlet–triplet energy gap ($\Delta E_{T-OS} = 1.21$ kcal/mol). The electron exchange coupling constant ($J = -1/2\Delta E_{T-OS}$) was estimated to be -211 cm^{-1} (Table S4), suggesting a weak interaction between the two radical centers. The spin density for $[1^{\bullet\bullet}]^{2-}$ is mainly localized on the two boron atoms (Table S5), indicating weak spin–spin couplings. The EPR spectra together with DFT calculations thus imply

that the formation of **4** may undergo a radical cyclization process similar to our previous diboryl compounds.⁴⁰ The thermal isomerization from complexes **4** to **5** may probably occur via a radical intermediate due to the cleavage of the B–C bond (Scheme S2a), which is similar to the reported light-driven isomerization.⁴⁶ Compared to $[1^{\bullet\bullet}]^{2-}$, $[2^{\bullet\bullet}]^{2-}$ and $[3^{\bullet\bullet}]^{2-}$ have triplet ground states with an even smaller singlet–triplet energy gap (Table S4). $[2^{\bullet\bullet}]^{2-}$ shows more spin density distribution delocalized to the adjacent naphthyl group (Table S5), while in the formation of **7**, the reaction path probably involves successive C–C coupling and similar “extrusion reaction”^{55,56} after radical cyclization, which leads to the departure of naphthalene derivatives (Scheme 4). The reaction mechanism for the formation of **8** has not been fully resolved so far and will be our future work.

CONCLUSION

In conclusion, we have synthesized a series of dicycloborate olefin complexes **4**–**7** from alkynyl-bridged diboryl compounds using a simple direduction strategy. In the reduction of **1**, temperature plays an important role in controlling the products (**4** and **5**). Meanwhile, a thermally driven isomerization was observed between complexes **4** and **5**. In addition, the formation of product **7**, although unexpected, indicates that with the choice of appropriate precursors, a variety of structures may be obtained utilizing effects like C–C coupling and “extrusion reaction”. Further studies of the reactivity, as well as the fluorescence properties of these anionic species, are underway.

EXPERIMENTAL SECTION

General Procedures. All reactions and manipulations were carried out under an argon atmosphere by using standard Schlenk techniques and a glovebox. $CDCl_3$ and CD_3CN were dried with 4 Å molecular sieve (2–3 days). Prior to use, the THF and Et_2O were dried by being refluxed with sodium and benzophenone and degassed by applying four freeze–pump–thaw cycles. The 1-bromo-2-ethynylbenzene,⁵⁷ 1,2-bis[2-(dimesitylboryl)phenyl]ethyne (**1**),⁴¹ 1,8-diiodonaphthalene,⁵⁸ 1,2-bis(8-bromonaphthalen-1-yl)ethyne,⁵⁹ and 1,8-bis[(2-bromophenyl)ethynyl]naphthalene⁶⁰ were synthesized according to literature methods. The 1H and ^{13}C NMR spectra were recorded using a JEOL JNM-ECS-400 or INOVA 600NB spectrometer (Bruker) at room temperature in parts per million downfield from Me_4Si . The ^{11}B NMR spectra were also recorded using a JEOL JNM-ECS-400 spectrometer at room temperature in parts per million downfield from external aqueous $BF_3 \cdot Et_2O$. The cyclic voltammetry experiment was conducted in an argon-filled atmosphere using a CHI 760e Electrochemical Workstation. Freshly

distilled THF was used as the solvent, and Bu_4NPF_6 (10^{-1} M) was used as the electrolyte. A standard three-electrode cell configuration was employed using a platinum-disk working electrode, a platinum-wire counter electrode, and a silver wire serving as the reference electrode. Formal redox potentials were referenced to the ferrocene/ferrocenium redox couple [$E(\text{Fc}/\text{Fc}^+) = 0$ V]. UV–visible–near-infrared (NIR) spectra were recorded on an Agilent Carry 5000 UV–vis–NIR spectrometer. Elemental analyses for C and H were carried out with a German Elementary Vario EL cube instrument.

X-ray Crystallography. The data were collected with a SuperNova (Dual) X-ray diffractometer equipped with Cu $K\alpha$ or Mo $K\alpha$ radiation ($\lambda = 1.54184$ or 0.71073 Å, respectively) at different temperatures (1 and 6, 173 K; 2, 4, and 5, 293 K; 3, 7, and 8, 150 K). Data reduction was performed using CrysAlis^{Pro} (version 1.171.37.35). The data sets were corrected by empirical absorption correction using spherical harmonics, implemented in the SCALE3 ABSPACK scaling algorithm.^{61,62} Crystal structures were determined by direct methods using Olex 2-1.2. Subsequent difference Fourier analyses and least-squares refinement with the SHELXL-2014/7 program package^{63–65} allowed for the location of the atom positions. Non-hydrogen atoms were refined with anisotropic displacement parameters during the final cycles. All hydrogen atoms were found in difference maps and refined using a riding model. More details about the crystallographic studies as well as atomic displacement parameters are given in CIF files. The crystallographic details for compounds 1–8 are summarized in Tables S1–S3. The data have been deposited in the Cambridge Crystallographic Data Centre (CCDC) with deposition numbers CCDC 1817515, 1817516, 1817518, 1817520–1817523, 1858155, and 1858156 for compounds 1–8, respectively. Despite repeated measurements, the quality of crystals of 6 and 7 was still not good enough. The uncertainties were relatively large and allowed for only a qualitative discussion. In addition, some residual electron density peaks (the maximum residual electron density peak at <1 e Å^{−3}) were found in the refinement of crystals 2 that have a strong influence on the *R* value, and we are not sure what solvents they are. Therefore, we use squeeze to delete these peaks, and the *R* values have been greatly reduced.

Computational Details. All the geometry optimizations were carried out at the UCAM-B3LYP/6-31G(d) level of theory. The obtained stationary points were characterized by frequency calculations. The broken-symmetry approach was applied for open-shell singlet calculations. All calculations were performed with the Gaussian 09 program suite.⁶⁶

EPR Measurements. Solution EPR measurements were carried out with a Bruker ER200DSRC10/12 spectrometer. A sample containing 10^{-3} M $[\text{I}^{\bullet}]^{2-}$ was prepared in a J. Young EPR tube inside a glovebox. The EPR spectrum was obtained at room temperature with a microwave power of 7.599 mW, a modulation amplitude of 0.5 G, a time constant of 81.92 ms, and a sweep time of 75 s. The EPR spectrum was simulated using EasySpin with hyperfine coupling constants.

Synthesis of 1,2-Bis[2-(dimesitylboranyl)phenyl]ethyne (1). Compound 1 was prepared according to ref 41. UV–vis–NIR (THF): 334 nm ($\log \epsilon = 4.16$). ¹H NMR (400 MHz, CDCl₃, 293 K): δ 7.14–7.20 (m, 6H, Ar-*H*), 6.73 (s, 8H, Ar-*H*), 6.58 (d, *J* = 8.0 Hz, 2H, Ar-*H*), 2.25 (s, 12H, Ar-CH₃), 1.93 (s, 24H, Ar-CH₃). ¹³C NMR (100 MHz, CDCl₃, 293 K): δ 149.8, 142.9, 140.8, 138.8, 134.0, 133.8, 133.2, 129.5, 128.3, 127.5, 127.3, 127.2, 93.5, 23.2, 21.4. ¹¹B NMR (128.3 MHz, CDCl₃, 293 K): δ 75.0.

Synthesis of 1,2-Bis[8-(dimesitylboranyl)naphthalen-1-yl]ethyne (2). Under anaerobic and anhydrous conditions, ^tBuLi (7.6 mL, 12.2 mmol, 1.6 M in hexanes) was added dropwise to a stirred THF solution of 1,2-bis(8-iodonaphthalen-1-yl)ethyne (3.18 g, 6.0 mmol) at -78 °C for 4 h, and then Mes₂BF (3.22 g, 12.0 mmol) in THF (15 mL) was slowly added. Subsequently, the reaction mixture was slowly warmed to room temperature and stirred overnight. After the addition of water, the solution was then extracted with dichloromethane. The crude product was then purified by column chromatography (10:1 CH₂Cl₂/hexanes) to afford 2 in 69% yield (3.20 g). Mp: 340–341 °C. UV–vis–NIR (THF): 337 nm ($\log \epsilon =$

4.38). ¹H NMR (300 MHz, CDCl₃, 293 K): δ 7.88 (d, *J* = 8.0 Hz, 2H, Ar-*H*), 7.82 (d, *J* = 8.0 Hz, 2H, Ar-*H*), 7.45 (d, *J* = 4.0 Hz, 2H, Ar-*H*), 7.36 (t, *J* = 8.0 Hz, 2H, Ar-*H*), 7.22 (d, *J* = 8.0 Hz, 2H, Ar-*H*), 6.73 (d, *J* = 8.0 Hz, 2H, Ar-*H*), 6.63 (s, 8H, Ar-*H*), 2.28 (s, 12H, -CH₃), 1.53 (broad, 24H, -CH₃). ¹³C NMR (100 MHz, CDCl₃, 293 K): δ 149.4, 138.7, 138.5, 136.3, 135.2, 133.6, 132.5, 130.1, 128.7, 126.0, 124.9, 122.7, 100.5 (alkyne quaternary carbon), 24.2, 21.5. ¹¹B NMR (128.3 MHz, CDCl₃, 293 K): δ 65.7. Elemental Anal. Calcd for C₅₈H₅₆B₂: C, 89.92; H, 7.29. Found: C, 89.84; H, 7.19.

Synthesis of 1,8-Bis[2-(dimesitylboranyl)phenyl]ethynyl-naphthalene (3). Under anaerobic and anhydrous conditions, ^tBuLi (7.6 mL, 12.2 mmol, 1.6 M in hexanes) was added dropwise to a stirred THF solution of 1,8-bis[2-(2-bromophenyl)ethynyl]naphthalene (2.90 g, 6.0 mmol) at -78 °C for 4 h, and then Mes₂BF (3.22 g, 12.0 mmol) in THF (15 mL) was slowly added. Subsequently, the reaction mixture was slowly warmed to room temperature and stirred overnight. After the addition of water, the solution was then extracted with dichloromethane. The crude product was then purified by column chromatography (10:1 CH₂Cl₂/hexanes) to afford 3 in 64% yield (3.16 g). Mp: 203.1–205.8 °C. UV–vis–NIR (THF): 337 nm ($\log \epsilon = 4.36$), 374 nm ($\log \epsilon = 4.08$). ¹H NMR (400 MHz, CDCl₃, 293 K): δ 7.64 (d, *J* = 8.0 Hz, 2H, Ar-*H*), 7.26–7.30 (m, 4H, Ar-*H*; the peaks of Ar-*H* were enwrapped in the peak of CDCl₃), 7.12–7.16 (m, 4H, Ar-*H*), 6.95 (t, *J* = 8.0 Hz, 2H, Ar-*H*), 6.74 (s, 8H, Ar-*H*), 6.57 (d, *J* = 8.0 Hz, 2H, Ar-*H*), 2.25 (s, 12H, -CH₃), 2.02 (s, 24H, -CH₃). ¹³C NMR (100 MHz, CDCl₃, 293 K): δ 149.9, 142.9, 140.9, 138.8, 135.1, 134.2, 133.6, 133.1, 131.1, 129.7, 128.9, 128.3, 127.8, 127.5, 124.7, 120.7, 97.6, and 93.2 (alkyne quaternary carbon), 23.2, 21.2. ¹¹B NMR (128.3 MHz, CDCl₃, 293 K): δ 74.1. Elemental Anal. Calcd for C₆₂H₅₈B₂: C, 90.29; H, 7.09. Found: C, 90.23; H, 7.00.

Synthesis of {[Na(Et₂O)₂]⁺·4a^{2−} (4). Under anaerobic and anhydrous conditions, a mixture of 1 (0.135 g, 0.20 mmol) and sodium (0.010 g, 0.44 mmol) in Et₂O was stirred at 10 °C for 3 days. The resultant light yellow solution was filtered to remove the dark insoluble substance. The filtrate was concentrated in vacuo, and a light yellow solid was obtained. Then the crude product was washed three times with hexanes, allowing for isolation of product 4. X-ray-quality light yellow crystals of 4 were obtained in an Et₂O solution at -25 °C. Yield: 0.118 g (58%). Mp: 209 °C (turn black). UV–vis–NIR (THF): 373 nm ($\log \epsilon = 3.83$), 329 nm ($\log \epsilon = 4.36$). ¹H NMR (400 MHz, CD₃CN, 293 K): δ 7.00 (d, *J* = 4.0 Hz, 2H, Ar-*H*), 6.59 (d, *J* = 8.0 Hz, 2H, Ar-*H*), 6.34–6.38 [m, 10H, Ar-*H* and Mes-*H*; the peaks of Ar-*H* (2H) were enwrapped in the peak of Mes-*H* (8H)], 6.30 (t, *J* = 8.0 Hz, 2H, Ar-*H*), 3.42 (q, *J* = 8.0 Hz, 16H, -OCH₂-), 2.07 (d, 36H, Ar-CH₃), 1.12 (t, *J* = 8.0 Hz, 24H, -OCH₂-CH₃). ¹³C NMR (150 MHz, CD₃CN, 293 K): δ 130.7, 130.2, 129.6, 128.8, 123.1, 122.3, 119.4, 118.7, 66.7 (Et₂O), 27.8, 21.3, 16.0 (Et₂O). ¹¹B NMR (128.3 MHz, CD₃CN, 293 K): δ −3.81. Elemental Anal. Calcd for C₆₆H₉₂B₂Na₂O₄: C, 77.94; H, 9.12. Found: C, 77.76; H, 9.04.

Synthesis of {[Na(Et₂O)₂]⁺·5a^{2−} (5). *Method A.* Under anaerobic and anhydrous conditions, a mixture of 1 (0.135 g, 0.20 mmol) and sodium (0.010 g, 0.44 mmol) in Et₂O was sealed and stirred at 40 °C for 4 days. The resultant golden yellow solution was filtered to remove the dark insoluble substance. The filtrate was concentrated in vacuo, and a golden yellow solid was obtained. Then the crude product was washed three times with hexanes, allowing for isolation of product 5. X-ray-quality golden yellow crystals of 5 were obtained in an Et₂O solution at -25 °C. Yield: 0.132 g (65%). *Method B.* Under anaerobic and anhydrous conditions, the Et₂O solution of 4 (0.102 g, 0.10 mmol) was sealed in a reactive tube. After being stirred at 40 °C for 2 days, the solution was concentrated in vacuo, and a golden yellow solid was obtained. Then the crude product was washed three times with hexanes, allowing for isolation of product 5. Yield: 0.089 g (87%). Mp: 281–283 °C. UV–vis–NIR (THF): 377 nm ($\log \epsilon = 4.40$), 329 nm ($\log \epsilon = 4.87$). ¹H NMR (400 MHz, CD₃CN, 293 K): δ 7.23 (d, *J* = 8.0 Hz, 2H, Ar-*H*), 7.08 (d, *J* = 8.0 Hz, 2H, Ar-*H*), 6.45 (t, *J* = 8.0 Hz, 2H, Ar-*H*), 6.34 (s, 8H, Ar-*H*), 6.23 (t, *J* = 8.0 Hz, 2H, Ar-*H*), 3.43 (q, *J* = 8.0 Hz, 16H, -OCH₂-), 2.06 (s, 24H, Ar-CH₃), 1.94 (broad, 12H, Ar-CH₃; the peaks of Ar-*H* were enwrapped in the peak of CD₃CN), 1.13 (t, *J* = 8.0 Hz, 24H, -OCH₂-

CH_3). ^{13}C NMR (100 MHz, CD_3CN , 293 K): δ 159.6, 142.1, 129.9, 128.8, 128.0, 122.3, 121.5, 118.6, 117.9, 65.9 (Et_2O), 26.9, 20.5, 15.2 (Et_2O). ^{11}B NMR (128.3 MHz, CD_3CN , 293 K): δ -7.98. Elemental Anal. Calcd for $\text{C}_{66}\text{H}_{92}\text{B}_2\text{Na}_2\text{O}_4$: C, 77.94; H, 9.12. Found: C, 77.75; H, 9.00.

Synthesis of the Mixture of 4 and 5. Under anaerobic and anhydrous conditions, a mixture of **1** (0.135 g, 0.20 mmol) and sodium (0.010 g, 0.44 mmol) in Et_2O was stirred at room temperature for 4 days. The resultant brownish yellow solution was filtered to remove the dark insoluble substance. The filtrate was concentrated in vacuo, and a yellow solid was obtained. Then the crude product was washed three times with hexanes, allowing for isolation of the solid. X-ray-quality yellow crystals were obtained in an Et_2O solution at -5°C . The ^1H NMR spectrum of the solid was recorded in CD_3CN at room temperature. The result shows the solid is a mixture of complexes **4** and **5**. In addition, the crystals were measured three times at a low temperature (110 K), and the results display the same disorder in the central core that consists of two configurations: bis-cycloborate olefin **4** and diborate-bridged stilbene structure **5**. This further shows the product is mixture of complexes **4** and **5**.

Synthesis of $\{[\text{K}(\text{THF})_2(18\text{-C-6})]^+\}_2\cdot 6\text{a}^{2-}$ (6**).** Under anaerobic and anhydrous conditions, a mixture of **2** (0.155 g, 0.20 mmol), 18-crown-6 (0.098 g, 0.40 mmol), and potassium (0.017 g, 0.44 mmol) in THF (≈ 35 mL) was stirred at room temperature for 3 h. The resultant yellowish-brown solution was filtered to remove the dark insoluble substance. The filtrate was concentrated in vacuo, and a yellow solid was obtained. Then the crude product was washed three times with hexanes, allowing for isolation of product **6**. X-ray-quality yellow crystals of **6** were obtained in a THF solution at room temperature. Yield: 0.243 g (73%). Mp: 158°C (turn black). UV-vis-NIR (THF): 450 nm ($\log \epsilon = 3.59$), 364 nm ($\log \epsilon = 4.05$), 310 nm ($\log \epsilon = 4.55$). ^1H NMR (400 MHz, CD_3CN , 293 K): δ 7.72 (dd, $J = 4.0$, 0.4 Hz, 2H, Ar-H), 7.08 (d, $J = 4.0$ Hz, 2H, Ar-H), 6.92–6.99 (m, 6H, Ar-H), 6.82 (t, $J = 8.0$ Hz, 2H, Ar-H), 6.03–6.49 (broad, 8H, Ar-H), 3.64 (t, 4H, -O-CH₂-), 3.57 (s, 48H, 18-C-6), 2.03–2.35 (broad, 36H, -CH₃), 1.80 (t, 4H, -O-CH₂-CH₂-). ^{13}C NMR (100 MHz, CD_3CN , 293 K): δ 156.4, 144.7, 131.6, 128.5, 127.7, 125.7, 125.1, 122.0, 121.4, 118.4, 117.8, 117.3, 70.0, 67.4, 26.3, 25.9, 19.8. ^{11}B NMR (128.3 MHz, CD_3CN , 293 K): δ -4.16. Elemental Anal. Calcd for $\text{C}_{82}\text{H}_{104}\text{B}_2\text{K}_2\text{O}_{12}\cdot\text{THF}$: C, 71.06; H, 7.77. Found: C, 70.95; H, 7.64.

Synthesis of $\{[\text{K}^+\cdot[2.2.2]\text{-cryptand}]\}_2\cdot 7\text{a}^{2-}$ (7**).** Under anaerobic and anhydrous conditions, a mixture of **3** (0.165 g, 0.20 mmol), [2,2,2]-cryptand (0.114 mg, 0.40 mmol), and potassium (0.017 g, 0.44 mmol) in THF (≈ 35 mL) was stirred at room temperature for 12 h. The resultant yellowish brown solution was filtered to remove the dark insoluble substance. The filtrate was concentrated in vacuo, and a yellow solid was obtained. Then the crude product was washed three times with hexanes, allowing for isolation of product **7**. X-ray-quality yellow crystals of **7** were obtained in a THF solution at room temperature. Yield: 0.131 g (43%). UV-vis-NIR (THF): 386 ($\log \epsilon = 4.00$), 421 nm ($\log \epsilon = 3.83$). ^1H NMR (400 MHz, CD_3CN , 293 K): δ 7.63 (d, $J = 8.0$ Hz, 2H, Ar-H), 7.63 (d, $J = 8.0$ Hz, 2H, Ar-H), 6.79 (t, $J = 8.0$ Hz, 6H, Ar-H), 6.67 (t, $J = 8.0$ Hz, 2H, Ar-H), 6.42 (s, 8H, Ar-H), 3.55 (s, 24H, Crypt ether), 3.50 (t, $J = 4.0$ Hz, 24H, Crypt ether), 2.52 (t, $J = 4.0$ Hz, 24H, Crypt ether), 2.24 (s, 12H, -CH₃). ^{11}B NMR (128.3 MHz, CD_3CN , 293 K): δ -2.50. Elemental Anal. Calcd for $\text{C}_{88}\text{H}_{124}\text{B}_2\text{K}_2\text{N}_4\text{O}_{12}\cdot\text{THF}$: C, 68.98; H, 8.31; N, 3.50. Found: C, 68.84; H, 8.23; N, 3.41. Note that this analysis was performed on hand-picked single crystals to ensure compound purity. The lack of a ^{13}C NMR spectrum is due to the poor solubility of complex **7**.

Synthesis of 1,2-Bis([Z]-2-(dimesitylboranyl)benzylidene)-1,2-dihydroacenaphthylene (8**).** Under anaerobic and anhydrous conditions, a mixture of **3** (0.165 g, 0.20 mmol) and sodium (0.010 g, 0.44 mmol) in Et_2O was stirred at room temperature for 12 h. The resultant yellowish-brown solution was filtered to remove the dark insoluble substance. Subsequently, 1 or 2 drops of H_2O was added to the filtrate, and a yellow solid was obtained. Then the crude product

was washed three times with hexanes, allowing for isolation of neutral product **8**. X-ray-quality yellow crystals of **8** were obtained in a THF solution at room temperature. Yield: 0.035 g (21%). Mp: 191.8°C (turn black). UV-vis-NIR (THF): 318 nm ($\log \epsilon = 4.57$), 414 nm ($\log \epsilon = 3.83$). ^1H NMR (400 MHz, CDCl_3 , 293 K): δ 7.47–7.52 (m, 6H, Ar-H), 7.36–7.42 (m, 4H, Ar-H), 7.14 (t, $J = 8.0$ Hz, 2H, Ar-H), 6.65 [s, 10H, Ar-H(2H)+Mes-H(8H)], 6.12 (s, 2H, =CH), 2.10 (s, 12H, -CH₃), 1.88 (s, 24H, -CH₃). ^{13}C NMR (100 MHz, CDCl_3 , 293 K): δ 146.7, 143.4, 142.3, 138.5, 136.8, 135.4, 135.3, 131.2, 130.8, 128.7, 128.1, 127.2, 127.0, 125.6, 123.8, 119.1, 23.2, 21.2. ^{11}B NMR (128.3 MHz, CDCl_3 , 293 K): δ 70.0. Elemental Anal. Calcd for $\text{C}_{62}\text{H}_{60}\text{B}_2$: C, 90.07; H, 7.32. Found: C, 90.04; H, 7.28.

■ ASSOCIATED CONTENT

Supporting Information

The Supporting Information is available free of charge on the ACS Publications website at DOI: 10.1021/acs.inorgchem.8b01555.

^1H , ^{13}C , and ^{11}B NMR spectra of compounds **1**–**8** and computational details (PDF)

Accession Codes

CCDC 1817515, 1817516, 1817518, 1817520, 1817521, 1817522, 1817523, 1858155, and 1858156 contain the supplementary crystallographic data for this paper. These data can be obtained free of charge via www.ccdc.cam.ac.uk/data_request/cif, or by emailing data_request@ccdc.cam.ac.uk, or by contacting The Cambridge Crystallographic Data Centre, 12 Union Road, Cambridge CB2 1EZ, UK; fax: +44 1223 336033.

■ AUTHOR INFORMATION

Corresponding Authors

*E-mail: boxb@lzu.edu.cn.

*E-mail: xingyong@uow.edu.au.

ORCID

Xingyong Wang: 0000-0002-6047-8722

Xiaobo Pan: 0000-0002-5757-2339

Jincai Wu: 0000-0002-8233-2863

Author Contributions

\ddagger J.Z. and C.R. contributed equally to this work and should be considered co-first authors.

Funding

This work has been supported by the National Natural Science Foundation of China (21771094 and 21671087) and the Fundamental Research Funds for the Central Universities (lzujbky-2017-k07). The authors also acknowledge the support from the Vice-Chancellor's Postdoctoral Research Fellowship Funding of the University of Wollongong and the computational resources provided by NCI's National Computational Merit Allocation Scheme.

Notes

The authors declare no competing financial interest.

■ ACKNOWLEDGMENTS

The authors sincerely appreciate Dr. Shengchun Wang for his useful discussion and suggestion.

■ REFERENCES

(1) Entwistle, C. D.; Marder, T. B. Boron chemistry lights the way: optical properties of molecular and polymeric systems. *Angew. Chem., Int. Ed.* **2002**, *41*, 2927.

- (2) Entwistle, C. D.; Marder, T. B. Applications of three-coordinate organoboron compounds and polymers in optoelectronics. *Chem. Mater.* **2004**, *16*, 4574.
- (3) Hudson, Z. M.; Wang, S. Impact of donor–acceptor geometry and metal chelation on photophysical properties and applications of triarylboranes. *Acc. Chem. Res.* **2009**, *42*, 1584.
- (4) Jäkle, F. Advances in the synthesis of organoborane polymers for optical, electronic, and sensory applications. *Chem. Rev.* **2010**, *110*, 3985.
- (5) Wakamiya, A.; Yamaguchi, S. Designs of functional π -electron materials based on the characteristic features of boron. *Bull. Chem. Soc. Jpn.* **2015**, *88*, 1357.
- (6) Mukherjee, S.; Thilagar, P. Stimuli and shape responsive ‘boron-containing’ luminescent organic materials. *J. Mater. Chem. C* **2016**, *4*, 2647.
- (7) Li, S.-Y.; Sun, Z.-B.; Zhao, C.-H. Charge-transfer emitting triarylborane π -electron systems. *Inorg. Chem.* **2017**, *56*, 8705.
- (8) Ji, L.; Griesbeck, S.; Marder, T. B. Recent developments in and perspectives on three-coordinate boron materials: a bright future. *Chem. Sci.* **2017**, *8*, 846.
- (9) Yamaguchi, S.; Akiyama, S.; Tamao, K. Tri-9-anthrylborane and its derivatives: new boron-containing π -electron systems with divergently extended π -conjugation through boron. *J. Am. Chem. Soc.* **2000**, *122*, 6335.
- (10) Wakamiya, A.; Mori, K.; Yamaguchi, S. 3-Boryl-2,2'-bithiophene as a versatile core skeleton for full-color highly emissive organic solids. *Angew. Chem., Int. Ed.* **2007**, *46*, 4273.
- (11) Elbing, M.; Bazan, G. C. A new design strategy for organic optoelectronic materials by lateral boryl substitution. *Angew. Chem., Int. Ed.* **2008**, *47*, 834.
- (12) Hudnall, T. W.; Chiu, C.-W.; Gabbai, F. P. Fluoride ion recognition by chelating and cationic boranes. *Acc. Chem. Res.* **2009**, *42*, 388.
- (13) Wade, C. R.; Broomsgrove, A. E. J.; Aldridge, S.; Gabbai, F. P. Fluoride ion complexation and sensing using organoboron compounds. *Chem. Rev.* **2010**, *110*, 3958.
- (14) Yamaguchi, S.; Akiyama, S.; Tamao, K. Colorimetric fluoride ion sensing by boron-containing π -electron Systems. *J. Am. Chem. Soc.* **2001**, *123*, 11372.
- (15) Yin, X.; Liu, K.; Ren, Y.; Lalancette, R.; Loo, A. Y.-L.; Jäkle, F. Pyridalthiadiazole acceptor-functionalized triarylboranes with multi-responsive optoelectronic characteristics. *Chem. Sci.* **2017**, *8*, 5497.
- (16) Rao, Y.-L.; Amarne, H.; Wang, S. Photochromic four-coordinate N,C-chelate boron compounds. *Coord. Chem. Rev.* **2012**, *256*, 759.
- (17) Ansorg, K.; Braunschweig, H.; Chiu, C.-W.; Engels, B.; Gamon, D.; Hügel, M.; Kupfer, T.; Radacki, K. The pentaphenylborole–2,6-lutidine adduct: a system with unusual thermochromic and photochromic properties. *Angew. Chem., Int. Ed.* **2011**, *50*, 2833.
- (18) Nagura, K.; Saito, S.; Fröhlich, R.; Glorius, F.; Yamaguchi, S. N-heterocyclic carbene boranes as electron-donating and electron-accepting components of π -conjugated systems. *Angew. Chem., Int. Ed.* **2012**, *51*, 7762.
- (19) Escande, A.; Ingleson, M. J. Fused polycyclic aromatics incorporating boron in the core: fundamentals and applications. *Chem. Commun.* **2015**, *51*, 6257.
- (20) von Grotthuss, E.; John, A.; Kaese, T.; Wagner, M. Doping polycyclic aromatics with boron for superior performance in materials science and catalysis. *Asian J. Org. Chem.* **2018**, *7*, 37.
- (21) Dou, C.; Saito, S.; Matsuo, K.; Hisaki, I.; Yamaguchi, S. A boron-containing PAH as a substructure of boron-doped graphene. *Angew. Chem., Int. Ed.* **2012**, *51*, 12206.
- (22) Saito, S.; Matsuo, K.; Yamaguchi, S. Polycyclic π -electron system with boron at its center. *J. Am. Chem. Soc.* **2012**, *134*, 9130.
- (23) Farrell, J. M.; Schmidt, D.; Grande, V.; Würthner, F. Synthesis of a doubly boron-doped perylene through NHC-borenium hydroboration/C–H borylation/dehydrogenation. *Angew. Chem., Int. Ed.* **2017**, *56*, 11846.
- (24) Barlett, R. A.; Power, P. P. X-ray crystal structure of the boron-stabilized carbanion $[\text{Li}(12\text{-crown-4})_2][\text{CH}_2\text{C}_6\text{H}_2(3,5\text{-Me}_2)(4\text{-B}\{2,4,6\text{-Me}_3\text{C}_6\text{H}_2\}_2)]\cdot\text{Et}_2\text{O}$: evidence for “Boron Ylide” character. *Organometallics* **1986**, *5*, 1916.
- (25) Olmstead, M. M.; Power, P. P.; Weese, K. J.; Doedens, R. J. Isolation and x-ray crystal structure of the boron methylidenide ion $[\text{Mes}_2\text{BCH}_2]^-$ (Mes = 2,4,6-Me₃C₆H₂): a boron-carbon double bonded alkene analog. *J. Am. Chem. Soc.* **1987**, *109*, 2541.
- (26) Power, P. P. Persistent and stable radicals of the heavier main group elements and related species. *Chem. Rev.* **2003**, *103*, 789.
- (27) Kaim, W.; Hosmane, N. S.; Zálaiš, S.; Maguire, J. A.; Lipscomb, W. N. Boron atoms as spin carriers in two- and three-dimensional systems. *Angew. Chem., Int. Ed.* **2009**, *48*, 5082.
- (28) Martin, C. D.; Soleilhavoup, M.; Bertrand, G. Carbene-stabilized main group radicals and radical ions. *Chem. Sci.* **2013**, *4*, 3020.
- (29) Braunschweig, H.; Dewhurst, R. D. Single, double, triple bonds and chains: the formation of electron-precise B–B bonds. *Angew. Chem., Int. Ed.* **2013**, *52*, 3574.
- (30) Su, Y.; Kinjo, R. Boron-containing radical species. *Coord. Chem. Rev.* **2017**, *352*, 346.
- (31) Kaim, W.; Schulz, A. p-Phenylenediboranes: mirror images of p-phenylenediamines. *Angew. Chem., Int. Ed. Engl.* **1984**, *23*, 615.
- (32) Schulz, A.; Kaim, W. Bor-organische redox systeme. *Chem. Ber.* **1989**, *122*, 1863.
- (33) Braunschweig, H.; Dyakonov, V.; Engels, B.; Falk, Z.; Hörl, C.; Klein, J. H.; Kramer, T.; Kraus, H.; Krummenacher, I.; Lambert, C.; Walter, C. Multiple reduction of 2,5-bis(borolyl)thiophene: isolation of a negative bipolaron by comproportionation. *Angew. Chem., Int. Ed.* **2013**, *52*, 12852.
- (34) Ji, L.; Edkins, R. M.; Lorbach, A.; Krummenacher, I.; Brückner, C.; Eichhorn, A.; Braunschweig, H.; Engels, B.; Low, P. J.; Marder, T. B. Electron delocalization in reduced forms of 2-(BMes₂)pyrene and 2,7-bis(BMes₂)pyrene. *J. Am. Chem. Soc.* **2015**, *137*, 6750.
- (35) Zheng, Y.; Xiong, J.; Sun, Y.; Pan, X.; Wu, J. Stepwise reduction of 9,10-bis(dimesitylboryl)anthracene. *Angew. Chem., Int. Ed.* **2015**, *54*, 12933.
- (36) Wang, L.; Fang, Y.; Mao, H.; Qu, Y.; Zuo, J.; Zhang, Z.; Tan, G.; Wang, X. An isolable diboron-centered diradical with a triplet ground state. *Chem. - Eur. J.* **2017**, *23*, 6930.
- (37) Yuan, N.; Wang, W.; Fang, Y.; Zuo, J.; Zhao, Y.; Tan, G.; Wang, X. Bis(boryl anion)-substituted pyrenes: syntheses, characterizations, and crystal Structures. *Organometallics* **2017**, *36*, 2498.
- (38) Hübner, A.; Kaese, T.; Diefenbach, M.; Endeward, B.; Bolte, M.; Lerner, H.-W.; Holthausen, M. C.; Wagner, M. A preorganized ditopic borane as highly efficient one- or two-electron trap. *J. Am. Chem. Soc.* **2015**, *137*, 3705.
- (39) Lorbach, A.; Bolte, M.; Lerner, H.-W.; Wagner, M. Dilithio 9,10-diborataanthracene: molecular structure and 1,4-addition reactions. *Organometallics* **2010**, *29*, 5762.
- (40) Yu, L.; Li, Y.; Wang, X.; Zhou, P.; Jiang, S.; Pan, X. Consecutive reduction, radical-cyclization, and oxidative-dehydrogenation reaction of ortho-substituted diboryl compounds. *Chem. Commun.* **2017**, *53*, 9737.
- (41) Bresner, C.; Haynes, C. J. E.; Addy, D. A.; Broomsgrove, A. E. J.; Fitzpatrick, P.; Vidovic, D.; Thompson, A. L.; Fallis, I. A.; Aldridge, S. Comparative structural and thermodynamic studies of fluoride and cyanide binding by PhBMes₂ and related triarylborane Lewis acids. *New J. Chem.* **2010**, *34*, 1652.
- (42) Wang, X. Y.; Yu, L. R.; Inakollu, V. S. S.; Pan, X. B.; Ma, J.; Yu, H. B. Molecular quantum dot cellular automata based on diboryl monoradical anions. *J. Phys. Chem. C* **2018**, *122*, 2454.
- (43) Kaese, T.; Hübner, A.; Bolte, M.; Lerner, H.-W.; Wagner, M. Forming B–B bonds by the controlled reduction of a tetraaryl-diborane(6). *J. Am. Chem. Soc.* **2016**, *138*, 6224.
- (44) Silva Valverde, M. F.; Schweyen, P.; Gisinger, D.; Bannenberg, T.; Freytag, M.; Kleeberg, C.; Tamm, M. N-heterocyclic carbene boranes as electron-donating and electron-accepting components of π -conjugated systems. *Angew. Chem., Int. Ed.* **2017**, *56*, 1135.

- (45) Arrowsmith, M.; Böhnke, J.; Braunschweig, H.; Gao, H.; Légaré, M.; Paprocki, V.; Seufert, J. Synthesis and reduction of sterically encumbered mesoionic carbene-stabilized aryldihaloboranes. *Chem. - Eur. J.* **2017**, *23*, 12210.
- (46) Araneda, J. F.; Neue, B.; Piers, W. E.; Parvez, M. Photochemical synthesis of a ladder diborole: a new boron-containing conjugate material. *Angew. Chem., Int. Ed.* **2012**, *51*, 8546.
- (47) Araneda, J. F.; Piers, W. E.; Sgro, M. J.; Parvez, M. Bronsted acid-catalyzed skeletal rearrangements in polycyclic conjugated boracycles: a thermal route to a ladder diborole. *Chem. Sci.* **2014**, *5*, 3189.
- (48) Barton, J. W.; Shepherd, M. K. Synthesis and rearrangements of 1, 1'-bis(benzocyclobutylidene) and its derivatives. *J. Chem. Soc., Perkin Trans. 1* **1987**, 1561.
- (49) Rosenthal, A. J.; Devillard, M.; Miqueu, K.; Bouhadir, G.; Bourissou, D. A phosphine-coordinated boron-centered Gomberg-type radical. *Angew. Chem., Int. Ed.* **2015**, *54*, 9198.
- (50) Kushida, T.; Yamaguchi, S. Boracyclophanes: modulation of the σ/π character in boron-benzene interactions. *Angew. Chem., Int. Ed.* **2013**, *52*, 8054.
- (51) Fukazawa, A.; Yamaguchi, E.; Ito, E.; Yamada, H.; Wang, J.; Irle, S.; Yamaguchi, S. Zwitterionic ladder stilbenes with phosphonium and borate bridges: intramolecular cascade cyclization and structure-photophysical properties relationship. *Organometallics* **2011**, *30*, 3870.
- (52) Fukazawa, A.; Yamada, H.; Yamaguchi, S. Phosphonium- and borate-bridged zwitterionic ladder stilbene and its extended analogues. *Angew. Chem., Int. Ed.* **2008**, *47*, 5582.
- (53) Zhao, X.; Gilbert, T. M.; Stephan, D. W. C-C Coupling by thermolysis of alkynyl phosphonium borates. *Chem. - Eur. J.* **2010**, *16*, 10304.
- (54) Grigsby, W. J.; Power, P. P. Isolation and reduction of sterically encumbered arylboron dihalides: novel boranediyl insertion into C-C σ -bonds. *J. Am. Chem. Soc.* **1996**, *118*, 7981.
- (55) Wong, H. N. C.; Ng, T. K.; Wong, T. Y. Arene syntheses by extrusion of heteroatoms from 7-heteroatom-bicyclo[2.2.1]heptene systems. *Heterocycles* **1983**, *20*, 1815.
- (56) Guziec, F. S., Jr.; San Filippo, L. J. Synthetically useful extrusion reactions of organic sulfur, selenium and tellurium compounds. *Tetrahedron* **1988**, *44*, 6241.
- (57) Alabugin, I. V.; Gilmore, K.; Patil, S.; Manoharan, M.; Kovalenko, S. V.; Clark, R. J.; Ghiviriga, I. Radical cascade transformations of tris(*o*-aryleneethynyls) into substituted benzo-[*a*]indeno[2,1-*c*]fluorenes. *J. Am. Chem. Soc.* **2008**, *130*, 11535.
- (58) Liu, X.; Yi, Q.; Han, Y.; Liang, Z.; Shen, C.; Zhou, Z.; Sun, J.; Li, Y.; Du, W.; Cao, R. A robust microfluidic device for the synthesis and crystal growth of organometallic polymers with highly organized structures. *Angew. Chem., Int. Ed.* **2015**, *54*, 1846.
- (59) Huang, X.; Zeng, L.; Zeng, Z.; Wu, J. Intramolecular domino electrophilic and thermal cyclization of *peri*-ethynylene naphthalene oligomers. *Chem. - Eur. J.* **2011**, *17*, 14907.
- (60) Wu, Y. T.; Hayama, T.; Baldrige, K. K.; Linden, A.; Siegel, J. S. Synthesis of fluoranthenes and indenocorannulenes: elucidation of chiral stereoisomers on the basis of static molecular bowls. *J. Am. Chem. Soc.* **2006**, *128*, 6870.
- (61) *CrysAlisPro*, version 171.34.44; Oxford Diffraction Ltd.: Oxfordshire, U.K., 2010.
- (62) Clark, R. C.; Reid, J. S. The analytical calculation of absorption in multifaceted crystals. *Acta Crystallogr., Sect. A: Found. Crystallogr.* **1995**, *51*, 887.
- (63) Dolomanov, O. V.; Bourhis, L. J.; Gildea, R. J.; Howard, J. A. K.; Puschmann, H. OLEX2 a complete structure solution, refinement and analysis program. *J. Appl. Crystallogr.* **2009**, *42*, 339.
- (64) Sheldrick, G. M. A short history of SHELX. *Acta Crystallogr., Sect. A: Found. Crystallogr.* **2008**, *64*, 112.
- (65) Sheldrick, G. M. SHELXT-Integrated space-group and crystal-structure determination. *Acta Crystallogr., Sect. A: Found. Adv.* **2015**, *71*, 3.
- (66) Frisch, M. J.; Trucks, G. W.; Schlegel, H. B.; Scuseria, G. E.; Robb, M. A.; Cheeseman, J. R.; Scalmani, G.; Barone, V.; Mennucci, B.; Petersson, G. A.; Nakatsuji, H.; Caricato, M.; Li, X.; Hratchian, H. P.; Izmaylov, A. F.; Bloino, J.; Zheng, G.; Sonnenberg, J. L.; Hada, M.; Ehara, M.; Toyota, K.; Fukuda, R.; Hasegawa, J.; Ishida, M.; Nakajima, T.; Honda, Y.; Kitao, O.; Nakai, H.; Vreven, T.; Montgomery, J. A., Jr.; Peralta, J. E.; Ogliaro, F.; Bearpark, M.; Heyd, J. J.; Brothers, E.; Kudin, K. N.; Staroverov, V. N.; Keith, T.; Kobayashi, R.; Normand, J.; Raghavachari, K.; Rendell, A.; Burant, J. C.; Iyengar, S. S.; Tomasi, J.; Cossi, M.; Rega, N.; Millam, J. M.; Klene, M.; Knox, J. E.; Cross, J. B.; Bakken, V.; Adamo, C.; Jaramillo, J.; Gomperts, R.; Stratmann, R. E.; Yazyev, O.; Austin, A. J.; Cammi, R.; Pomelli, C.; Ochterski, J. W.; Martin, R. L.; Morokuma, K.; Zakrzewski, V. G.; Voth, G. A.; Salvador, P.; Dannenberg, J. J.; Dapprich, S.; Daniels, A. D.; Farkas, O.; Foresman, J. B.; Ortiz, J. V.; Cioslowski, J.; Fox, D. J. *Gaussian 09*, revision D.01; Gaussian, Inc.: Wallingford, CT, 2013.